Photon statistics of light fields based on single-photon-counting modules

G. Li, T. C. Zhang, Y. Li, and J. M. Wang
State Key Laboratory of Quantum Optics and Quantum Optics Devices and Institute of Opto-Electronics, Shanxi University, Taiyuan, 030006 China
(Received 21 June 2004; published 11 February 2005)

Single-photon-counting modules (SPCM's), with their high quantum efficiency, have been widely used to investigate effectively the photon statistics of various light sources, such as the single-photon state and emission light from controlled molecules, atoms, and quantum dots. However, such SPCM's cannot distinguish the arrivals of one photon and two (or more than two) photons at a moment, which makes measurement correction in real experiments. We analyze the effect of SPCM's on photon statistics based on the Hanbury-Brown-Twiss configuration when the total efficiency and background are considered, and it shows that the measured second-order degree of coherence and Mandel Q factor for different quantum states, including single-photon states and squeezed vacuum states, are corrected in different forms. A way of determining the squeezing of a squeezed vacuum state based on single-photon detection is presented.

DOI: 10.1103/PhysRevA.71.023807 PACS number(s): 42.50.Ar, 42.50.Dv, 03.65.Ta

I. INTRODUCTION

Since the Hanbury-Brown-Twiss (HBT) experiment [1], photon statistical properties have been widely investigated and the early experiment was finished by using a photomultiplier tube (PMT). The nonclassical character of light fields, such as the photon antibunching effect, was observed based on HBT configurations by measuring the two-time photoelectronic correlation [2–6]. In recent years, because of the development of quantum information science, the generation of quantum states, especially single-photon states, has played an important role in the implementation of quantum cryptography [7] and quantum computation [8]. Single-photon sources have been produced by pumping single molecules [9], individual quantum dots [10], and color centers [11,12] and by the way of cavity-QED (cavity quantum electrodynamics) [13]. It was reported, recently, that deterministic single photons were demonstrated by one controlled atom [14]. Single-photon-counting modules (SPCM's) with high quantum efficiency and low dark count rate are widely used in modern quantum optics experiments to measure the second-order degree of coherence $g^{(2)}$ of light emitted from single atoms [13] and the Q factor of a triggered single-photon source radiation [9]. However, the SPCM cannot detect more than one photon per pulse within a time shorter than its dead time, which means that all photon number probabilities P_n with $n \geqslant 1$ are all detected as P_1. Thus we have to correct the measured results.

In this paper we analyze how such SPCM's affect photon statistics based on the HBT configuration. The overall quantum efficiency and the background are taken into account. The corrected second-order degree of coherence $g^{(2)}$ and Mandel Q factor are obtained. We investigate several light fields, including the coherent state, ideal single-photon state, thermal state, and squeezed vacuum state, and it shows that for different quantum states the corrections are different. The second-order degree of coherence $g^{(2)}$ is more sensitive to real experimental situations than the Mandel Q factor in most cases.

This paper is organized as follows: first we will give the basic model of detecting the second-order degree of coherence and Mandel Q factor in Sec. II. We then describe the influences of the correction of the SPCM, the detection efficiency, and the background on the coherent state, single-photon state, thermal state, and squeezed vacuum state in Sec. III. Numerical results are also presented. In Sec. IV we summarize the main points of the paper.

II. MODEL OF DETECTION

The second-order degree of coherence $g^{(2)}$ and Mandel Q factor are well known as the important parameters for characterizing the statistical properties of light fields. The parameters can be measured by the HBT scheme which is comprised of two detectors (D_1 and D_2) and a 50/50 lossless beam splitter (BS) (see Fig. 1). $|\psi\rangle$ is the input field which has an intrinsic photon distribution $P_{in}(n)$. In general, the joint detection probability of D_1 in Δt_1 at r_1, t_1 and D_2 in Δt_2 at r_2, t_2 is [15]

$$\begin{aligned} P_2(r_1,t_1;r_2,t_2)\Delta t_1\Delta t_2 &= P_1(r_1,t_1)\Delta t_1 P_2(r_2,t_2)\Delta t_2 \\ &\times[1+\lambda(r_1,t_1;r_2,t_2)], \end{aligned} \tag{1}$$

where $P_1(r_1,t_1)\Delta t_1$ is the detection probability of D_1 in the time interval Δt_1 at r_1,t_1 and $P_1(r_2,t_2)\Delta t_2$ is the detection probability of D_2 in the time interval Δt_2 at r_2,t_2.

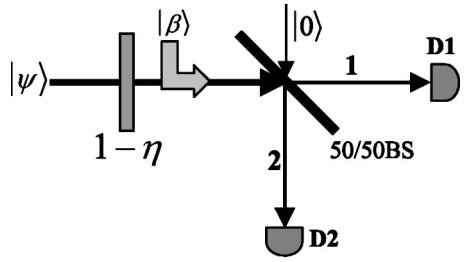

FIG. 1. HBT configuration with the detection efficiency η and coherent background $|\beta\rangle$.

$\lambda(r_1,t_1;r_2,t_2)$ is the normalized intensity correlation function, which can be expressed in term of the second-order degree of coherence $g^{(2)}(r_1,t_1;r_2,t_2)$:

$$\lambda(r_1,t_1;r_2,t_2) = g^{(2)}(r_1,t_1;r_2,t_2) - 1. \tag{2}$$

The second-order degree of coherence is then determined by the detected photon probabilities:

$$g^{(2)}(r_1,t_1;r_2,t_2) = \frac{P_2(r_1,t_1;r_2,t_2)}{P_1(r_1,t_1)P_2(r_2,t_2)}. \tag{3}$$

Set the time delay between the two detectors as $\tau=t_2-t_1=0$ for simplicity. Assume the two detectors are identical and have the same distances to the 50/50 lossless beam splitter. The detection probability of one detector and the joint detection probability of the two detectors can be written as $P_1=P_1(r_1,t_1)=P_1(r_2,t_2)$ and $P_2=P_2(r_1,t_1;r_2,t_2)$ in the case of statistical stationary fields. So the measured mean photon number of the incident field according to the measured photon probabilities is $\langle n\rangle=2P_1$. From Eq. (3), we have

$$g^{(2)} = P_2/P_1^2, \tag{4}$$

and the Mandel parameter can be written as [16]

$$Q = \frac{\langle(\Delta n)^2\rangle - \langle n\rangle}{\langle n\rangle} = \frac{4P_2(0)}{\langle n\rangle} - \langle n\rangle. \tag{5}$$

It is clear that the second-order degree of coherence and Mandel Q factor are determined by the joint detection probability of D_1 and D_2. Let us consider the real situation in experiment. Suppose the overall detection efficiency, including the optical collection efficiency, propagation efficiency, and quantum efficiency of photon detectors, is η. This overall efficiency can be regarded as an attenuation of the incident field by an attenuator with transmission of $(1-\eta)$. The background is another problem we have to face, which includes the environment radiation and the dark counts of the SPCM. Because the scattering background light from surroundings can be thought as a thermal field with very large bandwidth and very short coherent time (for example, even for a 1-nm bandwidth at wavelength of 500 nm, the coherent time is about 0.8 ps), the usual photon counting time (nanoseconds) discussed here is much longer than the coherent time and the photocounts of such time-average stationary background show a Poissonian distribution [15]. In a dark environment, the SPCM also generates random counts that follow a Poisson distribution. Both of these two random counts appear in the Poissonian distribution, and thus we can use a weak coherent field $|\beta\rangle$ with a Poissonian photon distribution $P(n)=\gamma^n e^{-\gamma}/n!$ with $\gamma=|\beta|^2$ [9,17] to simulate the backgrounds (see Fig. 1).

The photon number distribution after the attenuator is [15]

$$P_{tr}(m) = \sum_{n=m}^{\infty} \frac{n!}{m!(n-m)!}\eta^m(1-\eta)^{(n-m)}P_{in}(n); \tag{6}$$

then, the beam is mixed with the weak coherent background and the photon number distribution can be written as [18]

$$P_{mix}(l) = \sum_{m=0}^{l} \frac{\gamma^{(l-m)}}{(l-m)!}e^{-\gamma}P_{tr}(m). \tag{7}$$

The joint probability of detecting N photons on D_1 and $(l-N)$ photons on D_2 can be written as [19]

$$P(N,l-N) = \frac{l!}{N!(l-N)!}P_{mix}(l), \tag{8}$$

for ideal single-photon detectors. Yet the SPCM gives only one count within the dead time for one or more than one incident photon. The measured photon probabilities must be corrected. Actually, there are total four measured photon probabilities: $P(0,0)$, $P(0,1)$, $P(1,0)$, and $P(1,1)$. The detected joint probability of the two SPCM's, P_2, can be expressed as the sum of all probabilities that each detector has one count:

$$P_2 = P(1,1) = \sum_{l=2}^{\infty}\sum_{N=1}^{l-1}\left(\frac{1}{2}\right)^l \frac{l!}{N!(l-N)!}P_{mix}(l). \tag{9a}$$

The probability of having one count of one of the two detectors can be written as

$$P_1 = P(0,1) + P(1,1) = \sum_{l=1}^{\infty}\sum_{N=0}^{l}\left(\frac{1}{2}\right)^l \frac{l!}{N!(l-N)!}P_{mix}(l). \tag{9b}$$

The probability of none of the two detectors having photons is

$$P_0 = P_{mix}(0). \tag{9c}$$

III. NUMERICAL RESULTS FOR DIFFERENT FIELDS

A. Coherent field

Given the detection efficiency η and background $|\beta\rangle$, by use of Eqs. (9), a coherent incident field $|\varphi\rangle$ with a mean photon number $\alpha=|\varphi|^2$ gives

$$P_0 = e^{-(\eta\alpha+\gamma)}, \tag{10a}$$

$$P_1 = 1 - e^{-(\eta\alpha+\gamma)/2}, \tag{10b}$$

$$P_2 = (1 - e^{-(\eta\alpha+\gamma)/2})^2, \tag{10c}$$

$$\langle n\rangle = 2(1 - e^{-(\eta\alpha+\gamma)/2}). \tag{10d}$$

Equations (4) and (5) give $g^{(2)}=1$ and $Q=0$, which means that for coherent light, the measured results can characterize the statistical properties of the input light, and both the second-order degree of coherence and the Mandel factor are not affected by the total efficiency and background.

B. Single-photon field

If the incident field is a single-photon state—that is, $|1\rangle$—then, according to Eqs. (9), we get

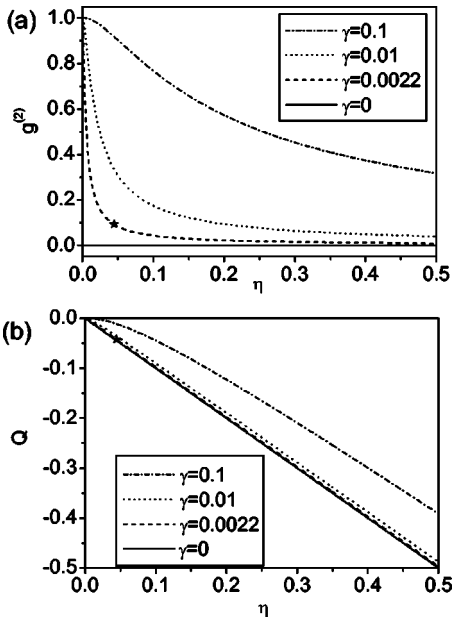

FIG. 2. The measured second-order degree of coherence $g^{(2)}$ (a) and Mandel Q factor (b) of the single-photon state as a function of overall efficiency η under different backgrounds: $\gamma=0$, 0.0022, 0.01, and 0.1. The star represents the experimental data in Ref. [9].

$$P_0 = (1-\eta)e^{-\gamma}, \tag{11a}$$

$$P_1 = \frac{1}{2}\left(1+\frac{1}{2}\eta\gamma e^{-\gamma}-(3-4\eta)e^{-\gamma}+(1-\eta)e^{-\gamma/2}\right), \tag{11b}$$

$$P_2 = 1+(1-2\eta)e^{-\gamma}-\frac{1}{2}\eta\gamma e^{-\gamma}-2(1-\eta)e^{-\gamma/2}, \tag{11c}$$

$$\langle n\rangle = 1+\frac{1}{2}\eta\gamma e^{-\gamma}-(3-4\eta)e^{-\gamma}+(1-\eta)e^{-\gamma/2}. \tag{11d}$$

The second-order degree of coherence $g^{(2)}$ and Mandel parameter Q can be given by Eqs. (4) and (5) accordingly.

Figure 2 shows $g^{(2)}$ and Q for the single-photon state as a function of the overall efficiency. It shows that the measured $g^{(2)}$ for an ideal single-photon source is strongly affected by the background and overall efficiency. Clearly, if there is no background, an ideal single photon will go to either detector 1 or detector 2 after the beam splitter and trigger only one of the detectors [20]. So the coincident probability of the two detectors in the HBT scheme is absolutely zero, which induces $g^{(2)}=0$ [solid line in Fig. 2(a)] and $Q=-\eta$ [solid line in Fig. 2(b)]. The background is a Poissonian distribution and gives the probabilities of two and more than two photons and would trigger the two detectors simultaneously and thus the stronger background gives a larger $g^{(2)}$ [Fig. 2(a)] and Mandel Q factor [Fig. 2(b)]. A lower detected efficiency is an equivalent of higher extra noise induced by losses, which is also random Poissonian, and consequently higher efficiency can reveal better the intrinsic photon statistics of the input field; here, for ideal one photon state, its $g^{(2)}$ is 0.

The star in Fig. 2 corresponds to the experimental data in Ref. [9]. In the experiment, the corresponding background is about $\gamma=0.0022$ and the overall efficiency is around $\eta=4.55\%$, which means for an ideal single-photon source the measured $g^{(2)}$ and Q should be about 0.09 and -0.04. If the overall efficiency improves to 50%, which is almost the best quantum efficiency at 850 nm of the present SPCM that we can get, then the results can reach to 0.009 and -0.5 accordingly.

For the low overall efficiency, such as 5% in actual experiments [9,13], the Mandel Q parameter is very close to zero. This Mandel Q factor cannot provide a distinct criterion to distinguish a single-photon field from a coherent source; on the other hand, the second-order degree of coherence is more convenient to distinguish a single-photon source when the overall efficiency cannot be effectively improved but the background is relatively low.

C. Thermal field

For incident single-mode thermal field the photon number satisfies the Bose distribution

$$P_n = \frac{\alpha^n}{(1+\alpha)^{n+1}}, \tag{12}$$

where α is the mean photon number of the thermal field. The measured photon probabilities and mean photon number when taking the efficiency and background into account are

$$P_0 = \frac{e^{-\gamma}}{1+\eta\alpha}, \tag{13a}$$

$$P_1 = \sum_{l=1}^{\infty}\sum_{N=1}^{l-1}\frac{l!}{N!\,(l-N)!}\left(\frac{1}{2}\right)^l\sum_{m=0}^{l}\frac{\gamma^{(l-m)}}{(l-m)!}e^{-\gamma} \times\sum_{n=m}^{\infty}\frac{n!}{m!\,(n-m)!}\eta^m(1-\eta)^{n-m}\frac{\alpha^n}{(1+\alpha)^{n+1}}, \tag{13b}$$

$$P_2 = \sum_{l=2}^{\infty}\sum_{N=1}^{l-1}\frac{l!}{N!\,(l-N)!}\left(\frac{1}{2}\right)^l\sum_{m=0}^{l}\frac{\gamma^{(l-m)}}{(l-m)!}e^{-\gamma} \times\sum_{n=m}^{\infty}\frac{n!}{m!\,(n-m)!}\eta^m(1-\eta)^{n-m}\frac{\alpha^n}{(1+\alpha)^{n+1}}, \tag{13c}$$

$$\langle n\rangle = 2P_1. \tag{13d}$$

If there is no background, we have

$$P_0 = \frac{1}{1+\eta\alpha}, \tag{14a}$$

$$P_1 = \frac{\eta\alpha}{2+\eta\alpha}, \tag{14b}$$

$$P_2 = \frac{(\eta\alpha)^2}{(2+\eta\alpha)(1+\eta\alpha)}, \tag{14c}$$

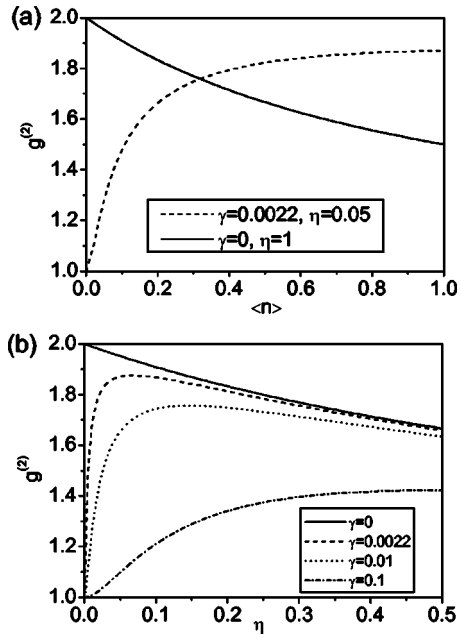

FIG. 3. The second-order degree of coherence $g^{(2)}$ via the measured mean photon number α (a) and detection efficiency η (b) for the thermal state.

$$\langle n\rangle = \frac{2\eta\alpha}{2+\eta\alpha}. \tag{14d}$$

If the overall efficiency is unity and the background is $|\beta\rangle$, we get

$$P_0 = \frac{e^{-\gamma}}{1+\alpha}, \tag{15a}$$

$$P_1 = 1 - \frac{2}{2+\alpha}e^{-\gamma/2}, \tag{15b}$$

$$P_2 = 1 - \frac{4}{2+\alpha}e^{-\gamma/2} + \frac{e^{-\gamma}}{1+\alpha}, \tag{15c}$$

$$\langle n\rangle = 2 - \frac{4}{2+\alpha}e^{-\gamma/2}. \tag{15d}$$

Figure 3 shows the second-order degree of coherence $g^{(2)}$ via the measured mean photon number $\langle n\rangle$ and detection efficiency η for thermal state. It is well known that for a single-mode thermal state the second-order degree of coherence is 2 and is independent of the mean photon number. Compared to the single-photon state and coherent state, the thermal state shows a bunching effect which means that the possibility of arrivals of multiphotons is higher than previous states and thus the measured results are affected even strongly by the SPCM since it cannot distinguish multiphoton. So we can see that even in the ideal case—i.e., $\gamma=0$ and $\eta=100\%$—the measured $g^{(2)}$ is not 2 any more. Actually, it decreases from 2 as the mean photon number increases since the probability of multiphotons is higher for a larger mean photon number [solid line in Fig. 3(a)]. When the background exists and the efficiency is not perfect, the overall result is that $g^{(2)}$ is increasing from 1 since the nonideal system corresponds a Possionian background with $g^{(2)}=1$ and so the mixed result is between 1 and 2 as we see in Fig. 3(a) (dashed line). The two effects, either from the SPCM itself or from the nonideal measurement, have different influences on the coincident counting and the measured mean photon number; consequently, when we see the $g^{(2)}$ as a function of efficiency [Fig. 3(b)], for a certain background (a mixed field) there exists a maximum value for a certain efficiency.

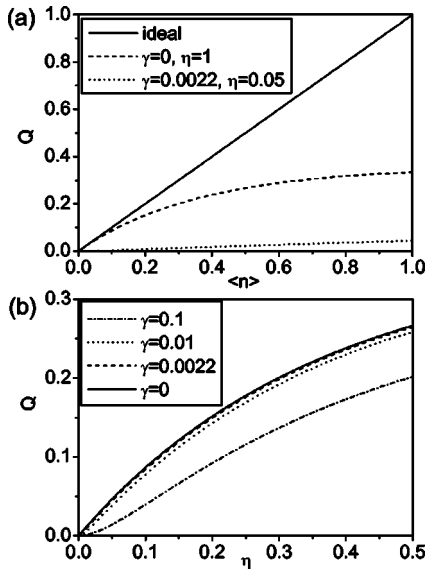

FIG. 4. Mandel parameter Q as a function of the measured mean photon number α (a) and the overall efficiency η (b) for the thermal field. In (b) the mean photon number $\alpha=1$.

The result of the Q factor is shown in Fig. 4. The *solid* line in Fig. 4(a) corresponds to the ideal result of the thermal field in theory—i.e., $Q=\langle n\rangle$. Similar to the above analysis for $g^{(2)}$, when the background exists the increase of Q is slow as the measured mean photon number [Fig. 4(a)] or the overall detection efficiency [Fig. 4(b)] increases. Higher background gives relatively low Q. Compared to the $g^{(2)}$, the Mandel Q factor is not a very sensitive parameter to the background.

D. Squeezed vacuum state

The squeezed vacuum state (SVS) is a very important and typical nonclassical state. It is defined as

$$|\xi\rangle = \hat{S}(\xi)|0\rangle, \tag{16}$$

where $\hat{S}(\xi)=\exp\left(\frac{1}{2}\xi^*\hat{a}^2-\frac{1}{2}\xi\hat{a}^{+2}\right)$ is the unitary squeeze operator with $\xi=r\exp(i\theta)$ and $r=|\xi|$ is the squeezed parameter. The photon number distribution of the squeezed vacuum state is [21]

$$P_{2n} = \frac{(\tanh r)^{2n}(2n)!}{\cosh r(n!\,2^n)^2}, \tag{17}$$

which clearly tells us that only an even number of photon distributions exists in this nonclassical field and it shows a bunching effect. The mean photon number, second-order de-

gree of coherence, and Mandel parameter of the SVS are obtained for a given squeezing parameter r in theory:

$$\langle n_{sq}\rangle = \sinh^2 r, \tag{18a}$$

$$g_{SVS}^{(2)} = 2 + \frac{\cosh^2 r}{\sinh^2 r}, \tag{18b}$$

$$Q_{SVS} = \sinh^2 r + \cosh^2 r. \tag{18c}$$

Similarly, from Eqs. (9), we get the measured photon probability based on the HBT configuration and SPCM's:

$$P_0 = e^{-r}\sum_{n=0}^{\infty}(1-\eta)^{2n}\frac{(\tanh r)^{2n}(2n)!}{\cosh r(n!2^n)^2}, \tag{19a}$$

$$P_1 = \sum_{l=1}^{\infty}\sum_{N=1}^{l-1}\frac{l!}{N!\,(l-N)!}\left(\frac{1}{2}\right)^l\sum_{m=0}^{l}\frac{\gamma^{(l-m)}}{(l-m)!}e^{-\gamma} \times \sum_{n=[(m+1)/2]}^{\infty}\frac{(2n)!}{m!(2n-m)!}\eta^m(1-\eta)^{2n-m}\frac{(\tanh r)^{2n}(2n)!}{\cosh r(n!2^n)^2}, \tag{19b}$$

$$P_2 = \sum_{l=2}^{\infty}\sum_{N=1}^{l-1}\frac{l!}{N!\,(l-N)!}\left(\frac{1}{2}\right)^l\sum_{m=0}^{l}\frac{\gamma^{(l-m)}}{(l-m)!}e^{-\gamma} \times \sum_{n=[(m+1)/2]}^{\infty}\frac{(2n)!}{m!\,(2n-m)!}\eta^m(1-\eta)^{2n-m}\frac{(\tanh r)^{2n}(2n)!}{\cosh r(n!2^n)^2}, \tag{19c}$$

$$\langle n\rangle = 2P_1. \tag{19d}$$

We can then use Eqs. (4) and (5) to get the results of the second-order degree of coherence and the Mandel parameter as the function of the squeezing parameter r and detection efficiency under different backgrounds. The numerical results are shown in Figs. 5 and 6.

Because for an ideal SVS there only exists the even photon number distribution and a very strong bunching effect is clearly shown, which implies large and sensitive corrections of statistical properties of the SVS measured by the SPCM in some cases. In fact the measured second-order degree of coherence $g^{(2)}$ is always bigger than 2 and is becoming small when r is getting larger [Fig. 5(a)]. $g^{(2)}$ is very sensitive to the efficiencies and backgrounds for lower squeezing, while for large squeezing it is not sensitive and the correction is very small. But in all these cases, the measured $g^{(2)}$ more or less reflects the real $g^{(2)}$ of the input SVS itself. This indicates that we can measure the squeezing of the SVS by measuring the $g^{(2)}$ in certain conditions when the correction is considered [Fig. 5(b)].

The properties of the Mandel Q factor of the SVS is also strongly corrected just by SPCM's [Fig. 6(b)]. According to Eq. (18c), the Q factor of the SVS increases along with the increasing of squeezing r, but from Fig. 6(a) we can see that the Q factor shows a decrease when the squeezing is increasing even in the case of perfect detection. If we take the overall efficiency and the background into account, the Q factor is very close to zero and does not change too much as squeezing increases. This shows that the measured Q factor is quite different from the real value of the input SVS. The results of Q are similar to the single-mode thermal state as both of them are bunching fields.

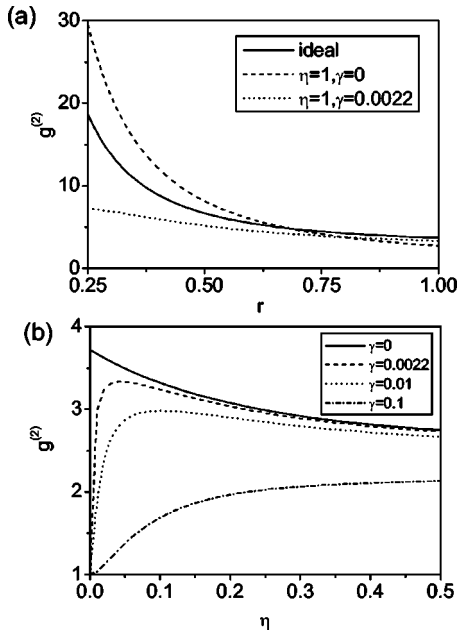

FIG. 5. The measured second-order degree of coherence $g^{(2)}$ of the squeezed vacuum state as a function of squeezing parameter r (a) and detection efficiency η (b) under different backgrounds and overall efficiencies. The squeezing parameter $r=1$ in (b).

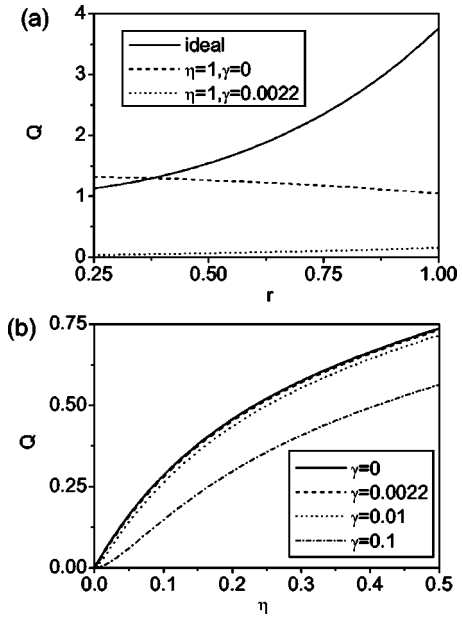

FIG. 6. Mandel Q factor of squeezed vacuum state as a function of squeezing parameter r (a) and overall efficiency η (b). The squeezing parameter $r=1$ in (b).

IV. CONCLUSION

We have discussed photon statistical properties based on the HBT experiment with SPCM's. The general result of the joint detection probability is obtained by taking the overall detection efficiency and background into account. The influence on second-order degree of coherence $g^{(2)}$ and the Mandel Q factor for various light fields, including the coherent state, single-photon state, thermal state, and squeezed vacuum state, are given analytically and numerically. It shows that for some quantum states, such as the single-photon state and squeezed vacuum state, the statistical properties are strongly corrected by SPCM's as well as the detection efficiency and background. Especially for well-investigated single-photon sources, which play an important role in quantum information, the correction of imperfect measurements and the SPCM itself must be considered. The measured $g^{(2)}$ for an ideal single-photon source is strongly affected by the background and overall efficiency, while the Mandel Q factor is not so sensitive to the background. But in the case of zero background, $g^{(2)}$ stays zero and is independent of the efficiency, whereas for the Mandel Q factor, it decreases linearly as the overall efficiency increases, $Q=-\eta$.

The photon statistics for the SVS is also investigated, and it shows that even in the case of ideal measurements—that is, 100% efficiency and no background—the SPCM has its correction to the photon statistics since the SPCM cannot tell the difference between one and more than one photon within its dead time. For some parameters, such as the Q factor of the SVS, the actual measured value is quite different from the value of the field itself. As the measured second-order degree of coherence of the SVS is sensitive to the squeezing parameter, one can determine the squeezing of the input SVS just by measuring $g^{(2)}$ under different detection efficiencies and backgrounds, instead of using the usual homodyne detection with strong local light.

With the help of multidetectors or fiber-optical setup the performance of single-photon detection can be improved [22], yet the two-port HBT configuration is still widely used in many quantum optics experiments. The analysis and method described in this paper could be extended to the situation of multiports to discuss, for example, the higher-order degree of coherence of light fields.

ACKNOWLEDGMENTS

This work is supported by the NSF of China under Grant Nos. 10434080, 10374062, and 60178006, the Research Funds for Youth from Shanxi Province (Grant No. 20031002), and Returned Scholars. T.C.Z. would like to thank Dr. L. T. Xiao for helpful discussions.

[1] H. Hanbury-Brown and R. Q. Twiss, Nature (London) **178**, 1046 (1956).
[2] H. J. Kimble, M. Dagenais, and L. Mandel, Phys. Rev. Lett. **39**, 691 (1977).
[3] F. Diedrich and H. Walther, Phys. Rev. Lett. **58**, 203 (1987).
[4] T. Basche, W. E. Moerner, M. Orrit, and H. Talon, Phys. Rev. Lett. **69**, 1516 (1992).
[5] F. De Martini, G. Di Giuseppe, and M. Marrocco, Phys. Rev. Lett. **76**, 900 (1996).
[6] C. Brunel, B. Lounis, P. Tamarat, and M. Prrit, Phys. Rev. Lett. **83**, 2722 (1999).
[7] N. Gisin, G. Ribordy, W. Tittel, and H. Zbinden, Rev. Mod. Phys. **74**, 145 (2002).
[8] H.-J. Briegel, S. J. van Enk, J. I. Cirac, and P. Zoller, in *The Physics of Quantum Information*, edited by D. Bouwmeester, A. Ekert, and A. Zeilinger (Springer, Berlin, 2000).
[9] F. Treussart, R. Alleaume, V. Le Floc'h, L. T. Xiao, J.-M. Courty, and J.-F. Roch, Phys. Rev. Lett. **89**, 093601 (2002).
[10] C. Santori, M. Pelton, G. Solomon, Y. Dale, and Y. Yamamoto, Phys. Rev. Lett. **86**, 1502 (2001).
[11] C. Kurtsiefer, S. Mayer, P. Zarda, and H. Weinfurter, Phys. Rev. Lett. **85**, 290 (2000).
[12] A. Beveratos, R. Brouri, T. Gacoins, A. Villing, J.-P. Poizat, and P. Grangier, Phys. Rev. Lett. **89**, 187901 (2002).
[13] J. McKeever, A. Baca, A. D. Boozer, J. R. Buck, and H. J. Kimble, Nature (London) **425**, 268 (2003).
[14] J. McKeever, A. Baca, A. D. Boozer, R. Miller, J. R. Buck, A. Kuzmich, and H. J. Kimble, Science **303**, 1992 (2004).
[15] L. Mandel and E. Wolf, *Optical Coherence and Quantum Optics* (Cambridge University Press, Cambridge, England, 1995).
[16] R. Short and L. Mandel, Phys. Rev. Lett. **51**, 384 (1983).
[17] L. T. Xiao, Y. T. Zhao, T. Huang, J. M. Zhao, W. B. Yin, and S. T. Jia, Chin. Phys. Lett. **21**, 489 (2004).
[18] J. A. Abate, H. J. Kimble, and L. Mandel, Phys. Rev. A **14**, 788 (1976).
[19] R. A. Campos, B. E. A. Saleh, and M. C. Teich, Phys. Rev. A **40**, 1371 (1989).
[20] P. Grangier, G. Roger, and A. Aspect, Europhys. Lett. **1**, 173 (1986).
[21] H.-A. Bachor, *A Guide to Experiments in Quantum Optics* (Wiley-VCH, New York, 1998).
[22] D. Achilles, C. Silberhorn, C. Sliwa, K. Banaszek, and Ian A. Walmsley, Opt. Lett. **28**, 2387 (2003); D. Achilles, C. Silberhorn, C. Sliwa, K. Banaszek, Ian A. Walmsley, M. J. Fitch, B. C. Jacobs, T. B. Pittman, and J. D. Franson, J. Mod. Opt. **51**, 1499 (2004).